

PROCEEDINGS OF SPIE

SPIDigitalLibrary.org/conference-proceedings-of-spie

Simulations of imperfect refractive index matching in scanning laser optical tomography and a method for correction

Ole Hill, Merve Wollweber, Roland Lachmayer, Tammo Ripken

Ole Hill, Merve Wollweber, Roland Lachmayer, Tammo Ripken, "Simulations of imperfect refractive index matching in scanning laser optical tomography and a method for correction," Proc. SPIE 12385, Three-Dimensional and Multidimensional Microscopy: Image Acquisition and Processing XXX, 1238509 (16 May 2023); doi: 10.1117/12.2649936

SPIE.

Event: SPIE BiOS, 2023, San Francisco, California, United States

Simulations of imperfect refractive index matching in Scanning Laser Optical Tomography and a method for correction

Ole Hill^a, Merve Wollweber^{a,b}, Roland Lachmayer^b, and Tammo Ripken^a

^aLaser Zentrum Hannover e.V., Hollerithallee 8, 30419 Hannover, Germany

^bLeibniz University Hanover, Welfengarten 1, 30167 Hannover, Germany

ABSTRACT

Since additive manufacturing has become increasingly popular in prototyping, printed optics are also beginning to enter the market. Novel characterization methods for printed optics are needed because traditional, destructive methods often do not work on these optics. The scope of investigation is also different for additively manufactured optics. Homogeneity of subtractively manufactured optics such as glass lenses is usually granted but for printed optics the interfaces in-between layers can cause absorption, scattering or refraction. Functionalised optics can also have characteristics such as fluorescence that cannot be tested with traditional methods.

The presented work tries to fill the void for this particular challenge by studying two non-destructive methods for optical characterisation of such components and expanding their use by clever combination. In Scanning Laser Optical Tomography (SLOT), a needle-like beam is formed and focused into the sample. The sample is scanned to form projection images and rotated to allow for reconstruction, which yields volumetric data about scattering, transmission and fluorescence of sample structures.

Simulated SLOT measurements with imperfect refractive index (RI) matching of sample and medium are presented. A method to correct distorted measurements is presented and evaluated. The simulations imply that a measurement with a RI mismatch of up to 0.1 can still yield reasonable results.

Keywords: tomography, digital microscopy, scanning laser optical tomography, optical coherence tomography, nondestructive

1. INTRODUCTION

Scanning Laser Optical Tomography (SLOT) is mostly utilized in biomedical imaging.^{1,2} It is a method best compared to Computer Tomography (CT) where an object is placed in a tube with a detection unit circling around it during image acquisition. Many projections are taken from different incident angles. Volumetric information is generated in a reconstruction process which usually involves a variation of filtered back projection.³

SLOT has two major differences compared to CT. The contrast mechanism is based on light instead of x-rays and it is the sample that is rotated instead of the detection unit. Further details and challenges of SLOT are described in chapter 2. With the use of light instead of x-rays comes the biggest obstacle of SLOT and comparable techniques like light sheet microscopy. While x-rays suffer very little refraction when travelling through typical CT media like human tissue,⁴ light rays are subject to strong refraction when passing media interfaces. This phenomenon is described in one of optics fundamental equation, namely Snell's law:⁵ $n_1 * \sin \alpha = n_2 * \sin \beta$, where n_1 and n_2 are the respective medium's RI and α is the incident angle and β is the exit angle. The issue of refraction is typically solved in imaging by surrounding the object with a medium that has the exact same RI as the sample, e.g. immersion objectives. This can be achieved by using the clearing agent used in clearing the object as an immersion medium. However, this is only possible for liquid and preferable nontoxic clearing agents. Protocols like CRYSTAL⁶ use an optical adhesive as the clearing agent which renders them unusable as an immersion medium. In SLOT it is necessary to fix the object in a transparent and hard material in order to

Further author information: (Send correspondence to Ole Hill)

Ole Hill: E-mail: o.hill@lzh.de, Telephone: 0049 511 2788388

Three-Dimensional and Multidimensional Microscopy: Image Acquisition and Processing XXX,
edited by Thomas G. Brown, Tony Wilson, Laura Waller, Proc. of SPIE Vol. 12385,
1238509 · © 2023 SPIE · 1605-7422 · doi: 10.1117/12.2649936

mount it on a rotary stage for data acquisition. Using the same material as an immersion medium is obviously not possible. Therefore, this issue is usually solved by using a silicone oil or a mixture of silicone oils with a closely matched RI. This solution does not come without drawbacks. Silicone oils can be costly and a palette of oils is necessary if a wide range of RI's is supposed to be covered because not all oils are mixable. Further issues concern toxicity and disposal of silicone oils which can increase overall cost even further. An approach which could reduce the necessity of RI matching is presented in this paper. It could allow data acquisition with imperfect RI matching of medium and sample by ray propagation simulation and reordering of image data.

2. THEORY AND METHODS

2.1 Scanning Laser Optical Tomography

SLOT is a digital imaging method usually used for fluorescent biological samples. The technique has similarities with CT with the main differences being the usage of light instead of Röntgen rays and the rotation of the sample instead of the detection unit. The implications of these differences, especially refraction of light, are subjects of this work. An explanation of the fundamentals of SLOT are essential to the understanding of the proposed improvements to the method. Therefore, the technique is explained in the following.

The sample is usually a few millimeters in size and needs to be solid in order to allow precise reliable rotation during measurement. Therefore, it is usually embedded in an optical adhesive in a tube-like shape in order to be inserted in a rotary stage. An optical adhesive is used as the final clearing agent when applying the CRYSTAL clearing protocol. An advantage of this clearing protocol is that the prepared sample is relatively easy to handle because of the hard, transparent tube which is formed by the optical adhesive. This tube-like shape is necessary for the rotation of the sample during image acquisition. The sample has to be surrounded by a medium with a similar RI to the sample because mismatches in RI lead to artefacts and data loss during acquisition. In order to achieve this, the sample is positioned inside a glass cuvette which is filled with the immersion medium which is usually a mixture of silicone oils.

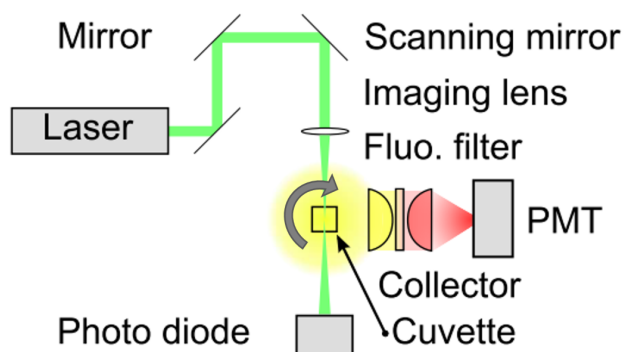


Figure 1: SLOT principle. A laser beam is scanned across a sample which is mounted on a rotation stage. A photo diode collects the transmitted light while the fluorescent light is focussed on a photo multiplier tube (PMT) which can be fitted with spectral filters.(modified from⁷)

Light is formed in a so-called needle beam which has a focal length matched to the diameter of the sample. The intensity of transmitted and fluorescent light is measured for every beam path. This data is correlated with the scanner position and results in a projection image. The intensity of transmitted light is measured by a photo diode behind the sample and the fluorescent light is measured from the side. The fluorescent light is collimated and filtered through interchangeable spectral filters before being recorded with a photo multiplier tube. The method is schematically depicted in figure 1. The resolution perpendicular to the beam is determined by the focusing optic and the resolution along the propagation of the beam is pseudo infinite, which leads to an anisotropic resolution very comparable to the projections of computer tomography. Several hundred projections are acquired over a full rotation of the sample. The result is a three dimensional sinogram of the acquired field of

view. This data can be reconstructed with filtered back projection to form cross sections of the sample containing locally resolved information about transmittance and fluorescence.⁷

This method works well if the RI of sample and medium is perfectly matched. But if there is a mismatch in RI, there is refraction at the border of the sample. This leads to a slightly altered real beam path compared to the expected beam path. The supposedly acquired data of each point does not match the actually acquired data. This leads to poor quality of the volumetric data.

2.2 Simulation Software

The SLOT simulation software is written in C++ using the Qt GUI library. Its goal is to visualize the effects of RI mismatches between the sample and the immersion medium. In order to achieve this, ray propagation simulations are performed for each projection angle. The input data consists of two cross sections of a sample where one only contains the boundary of the sample and the other contains a desired structure or pattern. In the following, the image of the boundary will be called input surface and the image of the structure will be called input structure.

Ray propagation

The incident rays are refracted when hitting an interface of changing RI, e.g. the sample surface. Snell's law is applied in this simulation. The RI of the sample and medium can be set to any value between 1 and 99. As the exit angle is of interest for the ray propagation, the missing input value for the equation is the incident angle. Therefore, the slope of the surface is determined by linear regression with a variable amount of considered neighbours.

The ray is then propagated through the cross section of the input structure. It is assumed that the sample has a constant RI and the rays are not refracted inside the sample. A bi-linear interpolation of the four closest neighbouring pixels of the sub-pixel position of the ray after it propagated the distance of one pixel is performed repetitively until the ray hits the surface on the backside. The gray values of these bi-linear interpolations are summed up to make up the brightness of the pixel of the incident position of the ray in the projection image. This propagation is repeated for each incident position of each projection angle and results in a sinogram of the input structure.

Rearrangement of sinogram

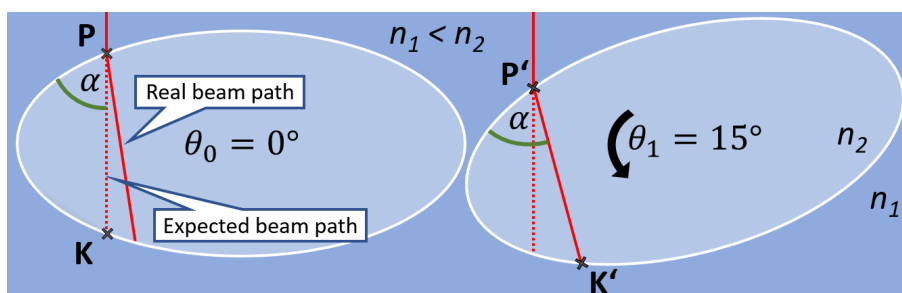


Figure 2: Left: The ray at incident point P is refracted because the RI of the medium n_1 is smaller than n_2 . The real beam path (RBP) is unequal to the expected beam path (EBP). α indicates the angle between the EBP and the sample surface. Right: After digitally rotating the sample by $\delta\theta$, the RBP at θ_1 (arbitrary) is equal to the EBP at θ_0 . α has the same value as on the left, but is the angle between the sample surface and the RBP at θ_1 .

Because the sample is rotated during data acquisition, there is information from almost every incident angle for each surface position. All of this data is saved in the sinogram of the input structure. When the RI is not matched, this information is simply at the wrong position. The goal of the rearrangement software is to correct these positioning errors by searching for the matching surface position and projection angle. Figure 2 tries to visualize the problem and the proposed solution. By digitally rotating the sample, the projection angle is found

where the incident position is hit by the ray in a way that the ray travels vertically through the sample at the original projection angle of the sample.

Before a rearrangement of the sinogram is possible, every rays' refraction angle for every projection angle has to be calculated. This is done by rotating the input surface to each projection angle and performing ray propagation calculations. This information is temporally saved in a multidimensional list called *entryPoints*. Excluding the cases where no refraction happens, either due to perfect match if RI's or a ray which is perpendicular to the sample surface, four different cases are plausible. They are depicted in figure 3. In any case where the exit angle gamma is negative (pointing to the left), the matching ray will be found by digitally rotating the sample clockwise. If the exit angle gamma is positive, the sample has to be digitally rotated counter-clockwise. The incident point is rotated step-wise (delta-theta) and the gamma of each of those steps is extracted from the *entryPoints*-list where the gamma of each incident point for each projection angle is saved. The matching data point is found when delta-theta is equal or larger than the gamma of said delta-theta projection angle at the rotated incident point.

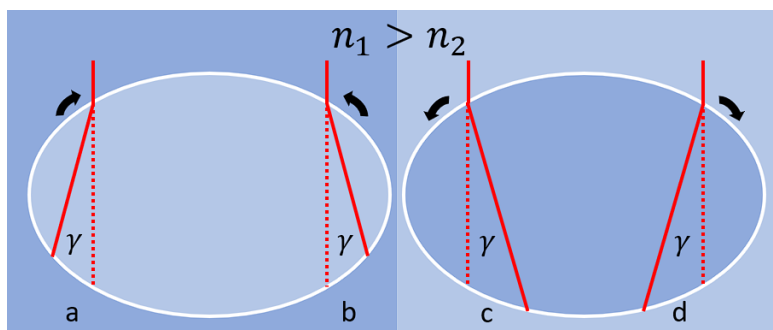


Figure 3: Four different cases of refraction (a, b, c, d). n_1 (darker blue) and n_2 (brighter blue) are RI's where $n_1 > n_2$. The black arrows indicate in which direction the sample has to be digitally rotated in order to find the matching data point in each refraction case.

Reconstruction

The simulated tomograms were reconstructed utilizing filtered back projection (fbp).³ Fiji,⁸ which is a library for ImageJ⁹ and the IMOD¹⁰ library were used in this process.

Data set

A hand drawn shape was used as the sample outline. Inside is the logo of the Laser Zentrum Hannover e.V. where bright parts represent high fluorescence signal. The input surface and input structure are illustrated in figure 4.

2.3 Quantitative Analysis

In an effort to evaluate the simulated results two methods of quantification were applied. The first method is known as structural similarity index measure (SSIM).¹¹ A SSIM plugin for ImageJ was used.¹² It is used to quantify how similar images appear to humans. The evaluation goes from zero, which would be a total mismatch between the images, to one, which would mean absolute similarity. The second method will be called absolute pixel difference (APD) in the following. For APD the difference in brightness of each pixel of the result compared to the expected image is taken and the average over the image or region of interested is calculated. Here, a value of zero would mean a perfect match. The maximum achievable value of 255 would be the case if one image was completely black and the other white.

The outer parts of tomographic images reconstructed with fbp are usually convoluted with artefacts. Because of this, both methods were applied to the object area and a few pixels around it. A second region of interest was set centrally in the object. Both areas are shown in figure 5.

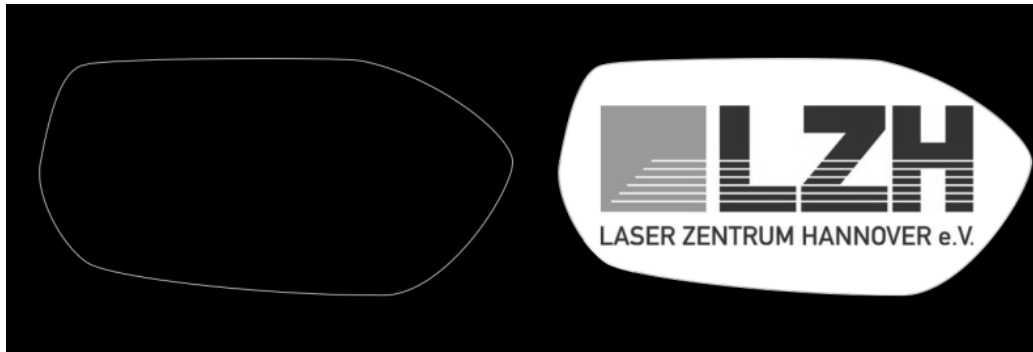


Figure 4: Input surface (left) and input structure (right) used for the simulated results in chapter 3. 8-bit gray value format with a resolution of 650x688 pixels each.

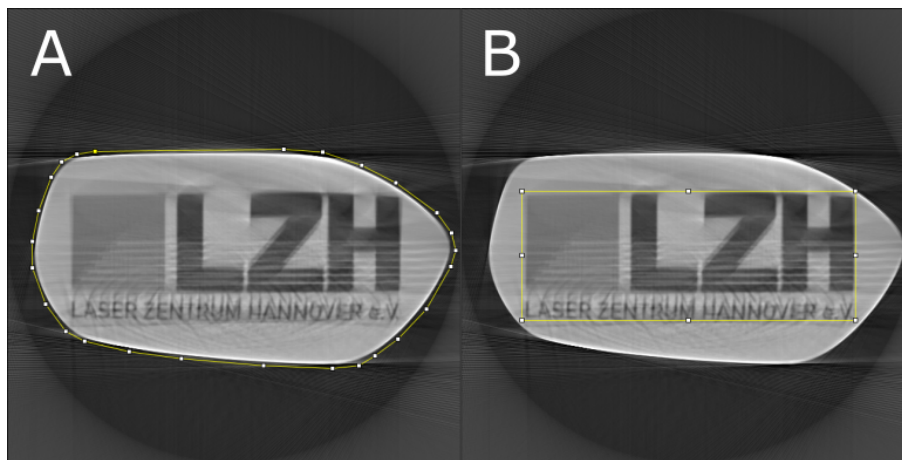


Figure 5: Two different regions of interested (ROI) were evaluated for each simulation. A shows the larger ROI which includes the entire cross section and a bit of background. B shows the smaller ROI which only includes the LZH logo. The typical ring artefact of tomograms is visible on the outside of the images.

3. RESULTS

The evaluation of the results of the simulations is split up into qualitative and quantitative analysis. It is important to make this distinction as different applications can have different requirements. For example, if a classification of tissue is done by a person, the structural similarity might be more important than the numerical similarity, e.g. contrast. But if a numerical analysis is performed, the brightness of individual pixels might be the deciding factor.

Qualitative analysis

Figure 6 shows reconstructions of simulations with different mismatches between medium and sample. The RI of the medium was 1.4 in all cases. 800 projections were performed for each result. Rows 1 and 3 show the results without correction while row 2 and 4 show results where a rearrangement of the sinogram based on ray propagation was performed. The lower two rows are zoomed in images of the upper ones, indicated by the red square. Column c) shows the result of reconstruction when no RI mismatch is present. The contrast in these images is the highest of all columns and the structure is best resolved.

It is clearly visible that a mismatch in RI is detrimental to the performance of SLOT if no correction is applied. The reconstructed outline of the sample as well as the inner structure is false. The improvement of image quality is remarkable when a rearrangement of the sinogram is performed. The comparison of 3a) and 4a)

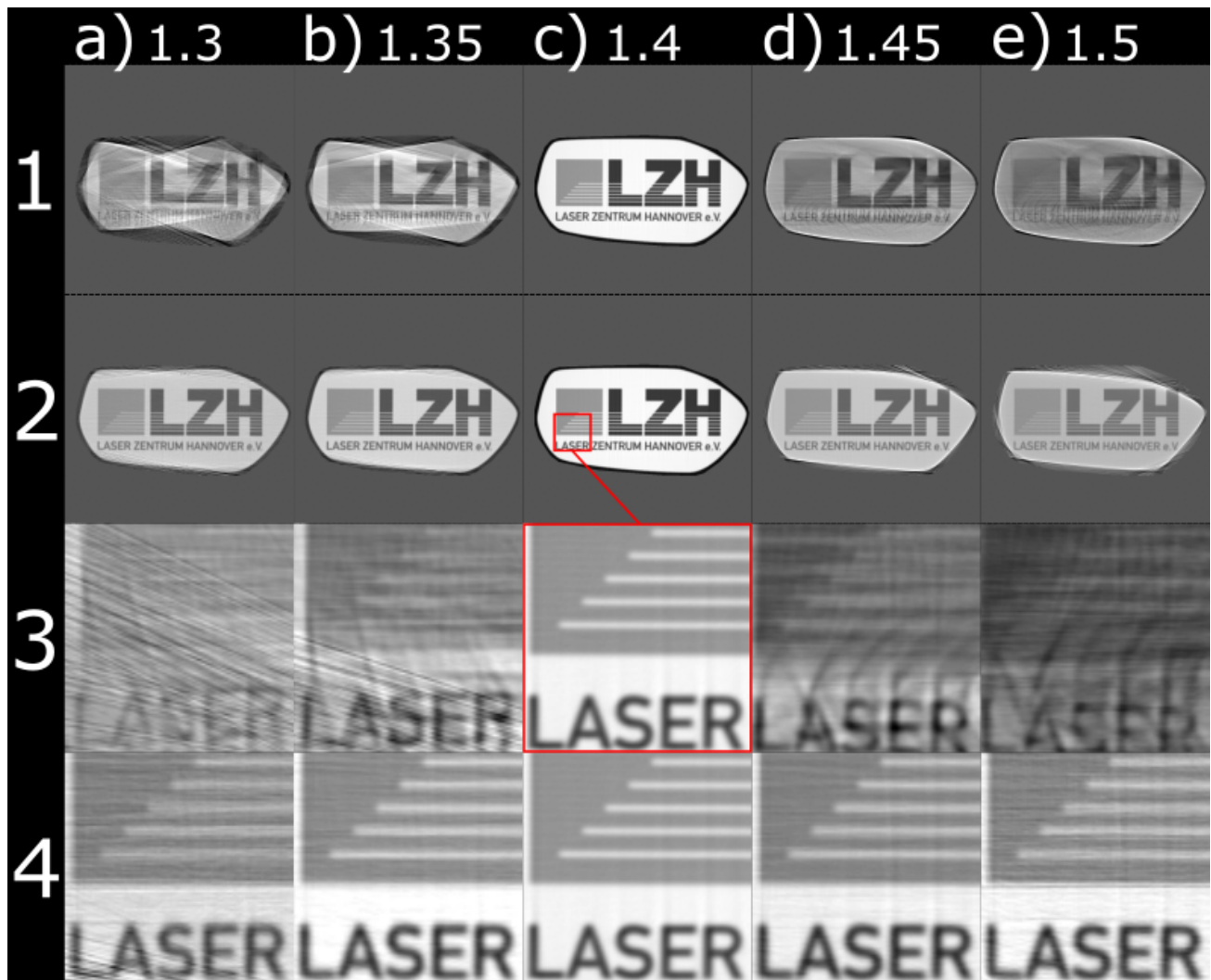


Figure 6: Comparison of reconstructions of different RI mismatches: The numeric values on top indicate the RI of the sample. The RI of the medium was 1.4 in all cases. Row 1 and 3 show reconstructions without correction of the sinogram. Row 2 and 4 show reconstructions where the sinogram was corrected for refraction. Row 3 and 4 display zoomed in images from row 1 and 2. 800 projections over one rotation were simulated for these images.

highlights the effects. In the uncorrected images, only the general brightness can be extracted from the result but in the corrected images almost all features of the source image are distinguishable.

Quantitative analysis

Figure 7 shows the results of absolute pixel difference (APD) which was applied to the images shown in figure 6 and additional simulations complementing the shown results with an increment of 0.01 mismatch in RI. The lower the value the higher the similarity to the result where no RI mismatch was present. The subjective improvement of the result shown in the previous chapter when the sinogram is rearranged is quantitatively confirmed here. Going back to the qualitative analysis, it is visible that the corrected images suffer a lower contrast which is homogeneous over the image. Meaning the main portion of the APD value results from the lower contrast and not from worse structural resolution. The performance of the rearrangement results in APD would be even greater if the contrast of the images would have been adjusted.

In contrast to APD, SSIM accounts more for structural similarity and less for total and regional differences

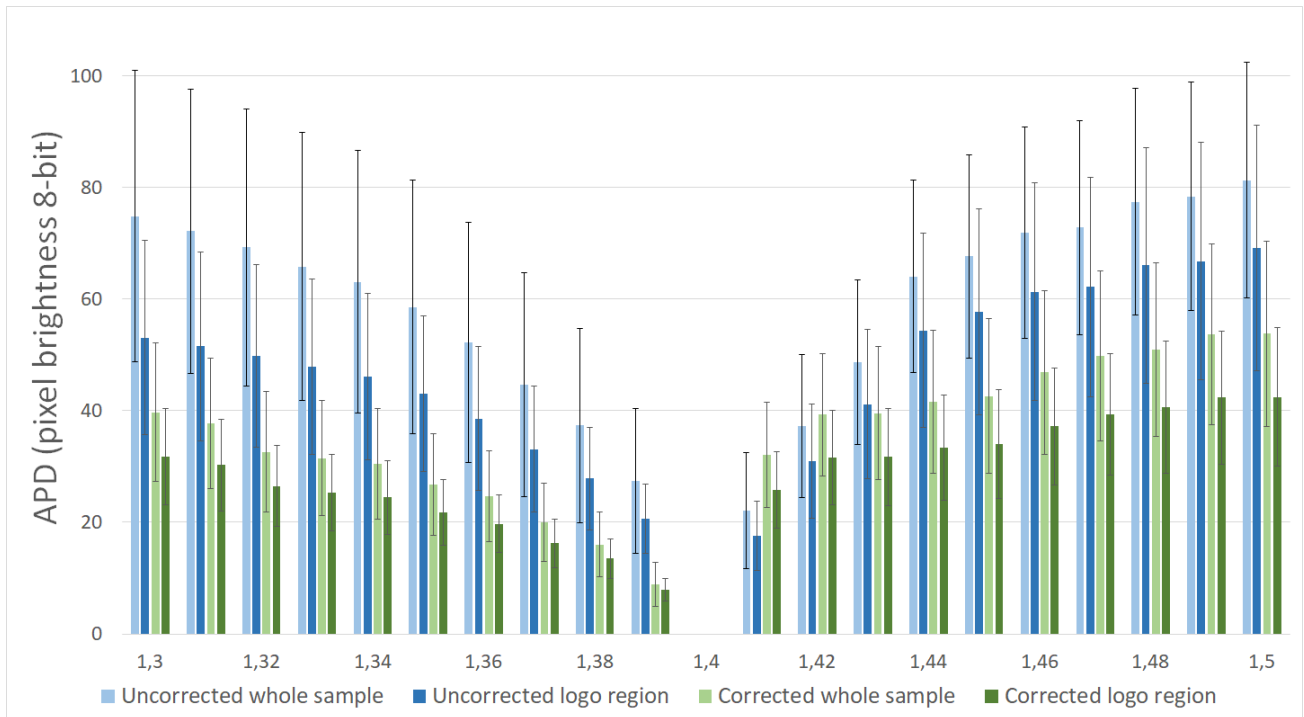


Figure 7: APD analysis of simulated reconstructions. The sample RI is indicated on the horizontal axis. The RI of the medium is 1.4 in all cases. The averaged APD over the respective region of interest and the standard deviation is shown. The ground truth image as well as the different regions of interest are depicted in figure 4 and 5

in brightness. The effect of this difference in evaluation is visible in figure 8. In the case of a mismatch of 1.4 (medium) to 1.3 (sample) the reconstruction of the corrected sinogram is twice as good as the uncorrected result when only looking the logo region of the sample.

An asymmetry regarding the RI mismatch is visible in the APD analysis when looking at values of the corrected images. A possible explanation for this is the strong refraction of light beams which hit the sample at the edges when a RI mismatch is present. Two different phenomena are present, depending on the type of RI mismatch.

In cases where the RI of the sample is smaller than the RI of the medium, the light gets refracted away from the center of the sample. This effect reduces the information density for the outer parts of a projection because neighbouring rays fan out. This can be viewed as a reduced sampling rate compared to parallel light rays. In extreme cases, total internal reflection can prevent the light ray from entering the sample all together. This leads to a dark spot in the sinogram and lower reconstruction quality even when digital correction is applied.

In cases where the RI of the sample is higher than the RI of the medium, the light gets refracted towards the middle of the sample. In extreme cases at the edge of the sample, this leads to a complete loss of information, which can not be corrected by the method presented in this paper. The presented method depends on the availability of data for each incident point and rotation angle. But if the rays at the edges of a sample get refracted too strongly towards the middle of the sample, no data for the outer incidents points is recorded. This is visible in figure 6 in image 2e) where the boundary of the sample is moved towards the center of the structure.

4. CONCLUSION

In this work an approach to correct SLOT data that is acquired with a mismatch in RI between sample and medium is presented. Simulations of uncorrected and rearranged measurements are compared. Evidence is presented that the correction works well and greatly improves the perceived image quality compared to uncorrected

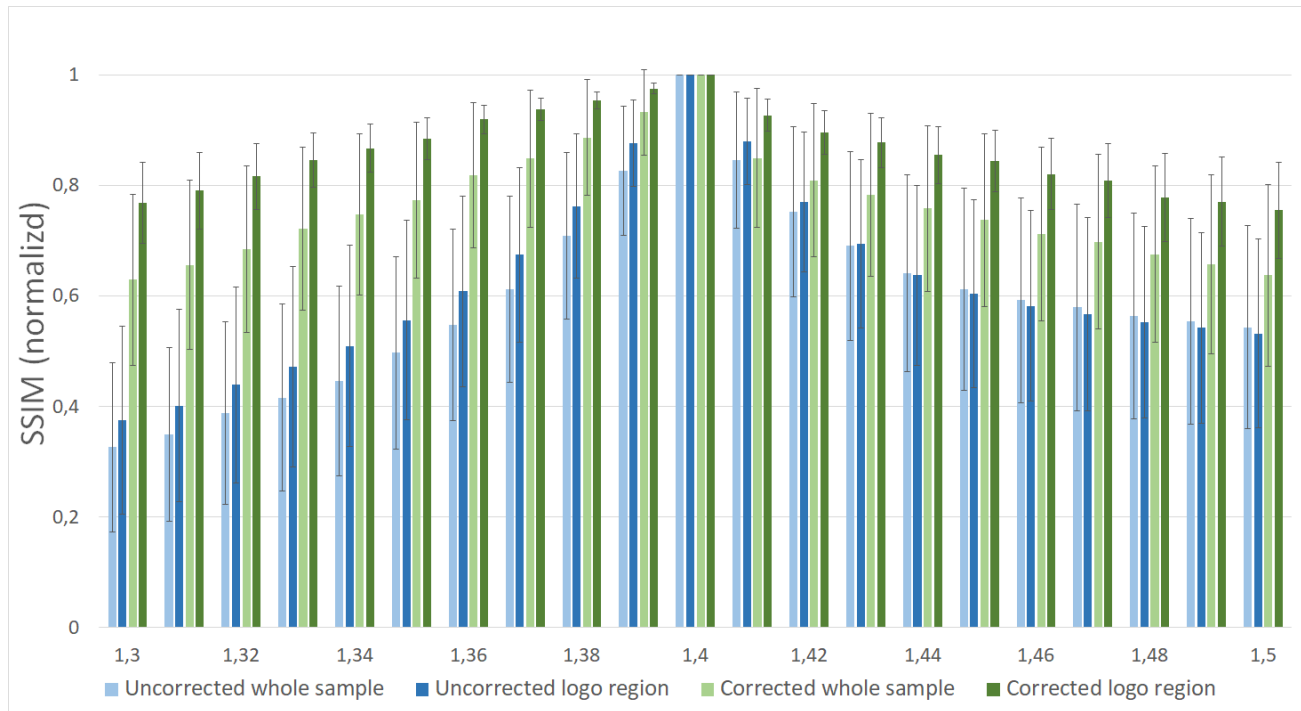


Figure 8: SSIM analysis of the same simulations as in figure 7. The greater the value the closer the evaluated image is to the reference image.

images. While the best result is still achieved when no RI mismatch is present, this approach could allow more freedom when choosing immersion media for SLOT. It could also reduce the need of precisely measuring the RI of sample and medium because these values can be adjusted in the rearrangement of the sinogram to achieve the highest image quality.

Acknowledgements

Funded by the Ministry for Science and Culture of Lower Saxony (MWK) – School for Additive Manufacturing SAM.

REFERENCES

- [1] Bode, K., Nolte, L., Kamin, H., Desens, M., Ulmann, A., Bergmann, G. A., Betker, P., Reitmeier, J., Ripken, T., Stern, M., Meyer, H., and Bicker, G., “Scanning laser optical tomography resolves developmental neurotoxic effects on pioneer neurons,” *Scientific Reports* **10**, 1–13 (2020).
- [2] Chen, L., Li, G., Tang, L., Zhang, M., Liu, L., Liu, A., McGinty, J., and Ruan, S., “Hyperspectral scanning laser optical tomography,” *Journal of Biophotonics* **12**, 1–9 (2019).
- [3] Kak, A. C. and Slaney, M., [*Principles of Computerized Tomographic Imaging*], SIAM (2001).
- [4] Attwood, D., [*Soft X-Rays and Extreme Ultraviolet Radiation: Principles and Applications - David Attwood - Google Books*], Cambridge University Press (1999).
- [5] Born, M. and Wolf, E., [*Principles of Optics*], Pergamin Press (1959).
- [6] Kellner, M., Heidrich, M., Lorbeer, R. A., Antonopoulos, G. C., Knudsen, L., Wrede, C., Izykowski, N., Grothausmann, R., Jonigk, D., Ochs, M., Ripken, T., Kühnel, M. P., and Meyer, H., “A combined method for correlative 3d imaging of biological samples from macro to nano scale,” *Scientific Reports* **6**, 1–12 (2016).
- [7] Lorbeer, R.-A., Heidrich, M., Lorbeer, C., Ojeda, D. F. R., Bicker, G., Meyer, H., and Heisterkamp, A., “Highly efficient 3d fluorescence microscopy with a scanning laser optical tomograph,” *Optics Express* **19**, 5419 (2011).

- [8] Schindelin, J., Arganda-Carreras, I., Frise, E., Kaynig, V., Longair, M., Pietzsch, T., Preibisch, S., Rueden, C., Saalfeld, S., Schmid, B., Tinevez, J. Y., White, D. J., Hartenstein, V., Eliceiri, K., Tomancak, P., and Cardona, A., "Fiji: An open-source platform for biological-image analysis," (7 2012).
- [9] Schneider, C. A., Rasband, W. S., and Eliceiri, K. W., "Nih image to imagej: 25 years of image analysis," (7 2012).
- [10] Kremer, J., Mastronarde, D., and McIntosh, R., "Computer visualization of three-dimensional image data using imod," *Journal of Structural Biology* **116**, 71–76 (1995).
- [11] Wang, Z., Bovik, A. C., Sheikh, H. R., and Simoncelli, E. P., "Image quality assessment: From error visibility to structural similarity," *IEEE Transactions on Image Processing* **13**, 600–612 (4 2004).
- [12] Renieblas, G. P., "Ssim index," (2008).